Laboratory Investigation (2018) 98:1170–1183
https://doi.org/10.1038/s41374-018-0081-0

ARTICLE

Attenuation of ventilation-induced diaphragm dysfunction through toll-like receptor 4 and nuclear factor-κB in a murine endotoxemia model

Li-Fu Li[1,2] · Yung-Yang Liu[3,4] · Ning-Hung Chen[1,2] · Yen-Huey Chen[5] · Chung-Chi Huang[1,2] · Kuo-Chin Kao[1,2] · Chih-Hao Chang[1] · Li-Pang Chuang[1] · Li-Chung Chiu[1]

Received: 21 December 2017 / Revised: 19 April 2018 / Accepted: 23 April 2018 / Published online: 20 June 2018

Abstract

Mechanical ventilation (MV) is often used to maintain life in patients with sepsis and sepsis-related acute lung injury. However, controlled MV may cause diaphragm weakness due to muscle injury and atrophy, an effect termed ventilator-induced diaphragm dysfunction (VIDD). Toll-like receptor 4 (TLR4) and nuclear factor-κB (NF-κB) signaling pathways may elicit sepsis-related acute inflammatory responses and muscle protein degradation and mediate the pathogenic mechanisms of VIDD. However, the mechanisms regulating the interactions between VIDD and endotoxemia are unclear. We hypothesized that mechanical stretch with or without endotoxin treatment would augment diaphragmatic structural damage, the production of free radicals, muscle proteolysis, mitochondrial dysfunction, and autophagy of the diaphragm via the TLR4/NF-κB pathway. Male C57BL/6 mice, either wild-type or TLR4-deficient, aged between 6 and 8 weeks were exposed to MV (6 mL/kg or 10 mL/kg) with or without endotoxemia for 8 h. Nonventilated mice were used as controls. MV with endotoxemia aggravated VIDD, as demonstrated by the increases in the expression levels of TLR4, caspase-3, atrogin-1, muscle ring finger-1, and microtubule-associated protein light chain 3-II. In addition, increased NF-κB phosphorylation and oxidative loads, disorganized myofibrils, disrupted mitochondria, autophagy, and myonuclear apoptosis were also observed. Furthermore, MV with endotoxemia reduced P62 levels and diaphragm muscle fiber size ($P < 0.05$). Endotoxin-exacerbated VIDD was attenuated by pharmacologic inhibition with a NF-κB inhibitor or in TLR4-deficient mice ($P < 0.05$). Our data indicate that endotoxin-augmented MV-induced diaphragmatic injury occurs through the activation of the TLR4/NF-κB signaling pathway.

Introduction

During the development of sepsis, bacterial components such as lipopolysaccharide (LPS) may mediate an inflammatory cascade and result in the release of inflammatory mediators, which can induce epithelial and endothelial injury, microvascular leakage, lung edema, and vasodilatation, subsequently leading to multiple organ system failure [1–8]. Moreover, sepsis may cause skeletal muscle atrophy due to increased protein breakdown via the ubiquitin–proteasome and autophagy–lysosomal pathways [4, 9]. Mechanical ventilation (MV) is often used to maintain life in patients with sepsis-related acute lung injury (ALI). However, controlled MV may result in diaphragmatic inactivity and rapid loss of diaphragm muscle strength and endurance, which is termed ventilator-induced diaphragm dysfunction (VIDD) [10–19]. Accumulating clinical evidence has revealed that mechanically ventilated

Electronic supplementary material The online version of this article (https://doi.org/10.1038/s41374-018-0081-0) contains supplementary material, which is available to authorized users.

✉ Li-Fu Li
lfp3434@cgmh.org.tw

1 Department of Internal Medicine, Division of Pulmonary and Critical Care Medicine, Chang Gung Memorial Hospital, Taoyuan, Taiwan

2 Department of Respiratory Therapy, Chang Gung Memorial Hospital, Taoyuan, Taiwan

3 Chest Department, Taipei Veterans General Hospital, Taipei, Taiwan

4 Institutes of Clinical Medicine, School of Medicine, National Yang-Ming University, Taipei, Taiwan

5 Department of Respiratory Care, College of Medicine, Chang Gung University, Taoyuan, Taiwan

septic patients frequently experience severe diaphragmatic weakness that may contribute to difficulties in ventilator weaning leading to further complications, such as ventilator-associated pneumonia, sepsis, and mortality [7, 8, 12, 20]. Therefore, the effect of interactions between sepsis and MV on diaphragm function must be investigated.

Sepsis-induced diaphragmatic dysfunction and VIDD appear to share several pathogenic mechanisms, including increased oxidative stress and mitochondrial dysfunction within the diaphragm muscle fibers, suggesting that sepsis may be an additional risk factor for VIDD [1, 7, 13, 21]. The onset of VIDD associated with decreased cross-sectional areas of slow-twitch and fast-twitch muscle fibers is rapid (within 6–8 h after the initiation of MV), and the magnitude of impairment of diaphragmatic contraction increases with time on the ventilator [10, 16, 18, 22]. MV-induced oxidative stress in the diaphragm is a crucial signaling event that leads to the activation of calpain, caspase-3, and the proteasome system [12, 13, 16, 18, 19]. The major oxidants in the diaphragm during MV are reactive oxygen species (ROS), which are found in the mitochondrion, sarcoplasmic reticulum, transverse tubes, sarcolemma, and cytosol [13, 16, 22, 23]. Rodent studies on VIDD have demonstrated that MV induced diaphragmatic injury through excessive production of ROS by activating protein oxidation, lipid peroxidation, and microtubule-associated protein light chain 3 (LC3), which results in diaphragm inactivity [6, 11, 24–26]. Moreover, endotoxin- and MV-mediated ROS may increase the production of inflammatory cytokines, including interleukin (IL)-6, macrophage inflammatory protein-2 (MIP-2), a functional homolog of IL-8 in rodents, and tumor necrosis factor-α (TNF-α) [3, 5, 9, 13, 18, 27]. These inflammatory mediators, which suppress diaphragmatic function during endotoxemia, can arise mostly from the diaphragm itself, with subsequent autocrine and paracrine actions on the skeletal muscle fibers [3].

The nuclear factor-κB (NF-κB) signaling pathway, a pivotal signal transducer for many inflammatory mediators, increases the expression of specific E3 ubiquitin ligases of the ubiquitin–proteasome system, atrogin-1, and muscle ring finger-1 (MuRF-1), which contribute to protein degradation of the diaphragm muscle in VIDD or sepsis [3, 9, 12, 19, 28]. Additionally, NF-κB plays a vital role in the induction of the intrinsic apoptotic pathway and autophagy associated with mitochondrial injury in the diaphragm [6, 19, 29]. Previous murine studies of endotoxemia demonstrated that toll-like receptor 4 (TLR4), an important mediator of organ dysfunction in sepsis, regulated diaphragm catabolism, chemokine production, and autophagy through upregulation of the NF-κB or p38 mitogen-activated protein kinase pathways [4, 30–32]. A recent murine study of MV also demonstrated that TLR4 signaling mediates skeletal muscle atrophy through increased production of cytokines in the diaphragm [18]. However, the relationships between diaphragmatic injury or atrophy induced by endotoxin and MV, NF-κB activation, and the TLR4 pathway remain unclear.

In this study, we explored the relationships between MV with or without endotoxin and TLR4 and NF-κB signaling by using a murine model of VIDD. We hypothesized that mechanical stretch with or without LPS treatment would augment diaphragmatic structural damage, the production of free radicals, muscle proteolysis, mitochondrial dysfunction, and autophagy of the diaphragm via the TLR4/NF-κB pathway.

Materials and methods

Experimental animals

Wild-type or TLR4-deficient C57BL/6 mice, weighing between 20 and 25 g, aged between 6 and 8 weeks, were obtained from Jackson Laboratories (catalog number 007227, Bar Harbor, ME, USA) and National Laboratory Animal Center (Taipei, Taiwan) [27]. Briefly, homozygotes mutants ($TLR4^{-/-}$) exhibit a defective response to LPS stimulation [27]. Tlr4-deficient mice for the Tlr4Lps-del mutation display significantly reduced expression of proinflammatory genes compared to the controls [27]. The Tlr4Lps-del spontaneous mutation corresponds to a 74,723 bp deletion that completely removes the Tlr4 coding sequence. The null expressions of the TLR4 gene expression in $TLR4^{-/-}$ mice were confirmed by using a real-time polymerase chain reaction (PCR) analysis (Supplementary Fig. 1). We performed the experiments in accordance with the National Institutes of Health (NIH) Guidelines on the Use of Laboratory Animals. The Institutional Animal Care and Use Committee of Chang Gung Memorial Hospital approved the protocol (Permit number: 2015101201). All surgery was performed under zoletil and xylazine anesthesia, and all efforts were made to minimize suffering.

Experimental groups

Animals were randomly distributed into eight groups in each experiment: group 1, nonventilated control wild-type mice with normal saline; group 2, nonventilated control wild-type mice with LPS; group 3, tidal volume (V_T) 6 mL/kg wild-type mice with LPS; group 4, V_T 10 mL/kg wild-type mice with normal saline; group 5, V_T 10 mL/kg wild-type mice with LPS; group 6, V_T 10 mL/kg wild-type mice after SN50 administration with LPS; group 7, nonventilated control $TLR4^{-/-}$ mice with LPS; group 8, V_T 10 mL/kg

$TLR4^{-/-}$ mice with LPS. In each group, three mice underwent transmission electron microscopy (TEM) and five mice underwent measurement for cross-sectional area of the muscle fibers, immunohistochemistry assay, inflammatory cytokines, malondialdehyde (MDA), protein carbonyl groups, total antioxidant capacity, superoxide dismutase, terminal deoxynucleotidyl transferase-mediated dUTP-biotin nick end-labeling (TUNEL) assay, and Western blots.

Ventilator protocol

We used our established murine model of VILI, as described previously [18, 33]. Briefly, a 20-gauge angiocatheter was introduced into the tracheotomy orifice of mice and general anesthesia was maintained by regular intraperitoneal administration of zoletil 50 (5 mg/kg) and xylazine (5 mg/kg) at the beginning of the experiment and every 30 min. The mice were placed in a supine position on a heating blanket and then attached to a Harvard apparatus ventilator, model 55-7058 (Harvard Apparatus, Holliston, MA, USA), set to deliver 6 or 10 mL/kg at a rate of 100 breaths per min, for 8 h while breathing room air with zero end-expiratory pressure. At the end of the study period, heparinized blood was taken from the arterial line for analysis of arterial blood gas, and the mice were sacrificed. The nonventilated control mice were anesthetized and sacrificed immediately.

LPS and SN50 administration

Mice received either 1 mg/kg of Salmonella typhosa LPS (Lot 81H4018; Sigma Chemical Co., St. Louis, MO, USA) or an equivalent volume of normal saline intravenously via the internal jugular vein as a control. After 1 h of spontaneous respiration to allow for development of a septic response, the mice were subjected to MV for 8 h. The dose was chosen based on previous in vivo study of our coworkers that showed 1 mg/kg LPS induced mild endotoxemia [34]. SN50 is a NF-κB inhibitor (2 mg/kg; Calbiochem, San Diego, CA, USA) and was given intraperitoneally 30 min before MV based on our present and previous studies that showed 2 mg/kg inhibited NF-κB activity [19].

Measurement of cytokines in the bronchoalveolar lavage fluid

IL-6 with a lower detection limit of 1.8 pg/mL and MIP-2 (1 pg/mL) were detected in the bronchoalveolar lavage (BAL) fluid using immunoassay kits containing primary polyclonal anti-mouse antibodies that were cross-reactive with rat and mouse IL-6 and MIP-2 (Biosource International, Camarillo, CA, USA). Each sample was run in duplicate according to the manufacturer's instructions.

Measurement of diaphragmatic oxidative stress and antioxidant enzyme expression

The diaphragms were homogenized in phosphate buffered saline. The protein carbonyl groups, MDA, total antioxidant capacity, and superoxide dismutase in the protein extracts were measured using the OxiSelect protein carbonyl assay kit containing dinitrophenylhydrazine, Oxiselect TBARS assay kit containing thiobarbituric acid reactive substances, Oxiselect total antioxidant capacity assay kit containing uric acid, and Oxiselect superoxide dismutase assay kit containing xanthine/xanthine oxidase system (Cell Biolabs, San Diego, CA, USA). Each sample was run in duplicate and expressed as μmol/g protein for protein carbonyl groups, MDA, and superoxide dismutase, and μmol copper reducing equivalents/g protein for total antioxidant capacity according to the manufacturer's instructions.

Immunoblot analysis

The diaphragms were homogenized in 1 mL of lysis buffer (20 mM HEPES pH 7.4, 1% Triton X-100, 10% glycerol, 2 mM ethylene glycol-bis (β-aminoethyl ether)-*N*, *N*, *N*′, *N*′-tetraacetic acid, 50 μM β-glycerophosphate, 1 mM sodium orthovanadate, 1 mM dithiotreitol, 400 μM aprotinin, and 400 μM phenylmethylsulfonyl fluoride), transferred to eppendorf tubes and placed on ice for 15 min. The tubes were centrifuged at 15,350×*g* for 10 min at 4 °C and the supernatant was flash-frozen. The total protein concentration was detected by Bradford protein assay kit (Thermo Fisher Scientific Inc., Waltham, MA, USA). Crude cell lysates related to the total protein content (phosphorylated and non-phosphorylated correct to input) were matched for protein concentration (30 μg per well for caspase-3 and LC3-II; 60 μg per well for atrogin-1, MuRF-1, phosphorylated NF-κB, and TLR4; 100 μg per well for P62 and phosphorylated inhibitor-κBα (IκBα)), resolved on a 10% bis-acrylamide gel, and electrotransferred to Immobilon-P membranes (Millipore Corp., Bedford, MA, USA). For the assay of TLR4, phosphorylated NF-κB, phosphorylated IκBα, NF-κB, IκBα, caspase-3, atrogin-1, MuRF-1, LC3-II, P62, and glyceraldehydes-phosphate dehydrogenase, Western blot analyses were performed with respective antibodies (New England BioLabs, Beverly, MA, USA and Santa Cruz Biotechnology, Santa Cruz, CA, USA). Blots were developed by enhanced chemiluminescence (NEN Life Science Products, Boston, MA, USA).

Immunohistochemistry

The diaphragms were paraffin embedded, sliced at 4 μm, deparaffinized, antigen unmasked in 10 mM sodium citrate (pH 6.0), incubated with rabbit TLR4 primary antibody (1:100; Santa Cruz Biotechnology, Santa Cruz, CA, USA), and biotinylated goat anti-rabbit secondary antibody (1:100) according to the manufacturer's instruction for an immunohistochemical kit (Santa Cruz Biotechnology, Santa Cruz, CA, USA). The specimens were further conjugated with horseradish peroxidase–streptoavidin complex, detected with a diaminobenzidine (DAB) substrate mixture, and counterstained by hematoxylin. A dark-brown DAB signal, identified by arrows, indicated positive staining of TLR4 of muscle fibers, whereas shades of light blue signified nonreactive cells.

Cross-sectional area of the muscle fibers

The diaphragms were paraffin embedded, sliced at 4 μm, and stained with hematoxylin and eosin (H&E). The cross-sectional areas, a semi-quantitative method, were reviewed from 50 muscle fibers by a single investigator blinded to the therapeutic category of the mouse and then analyzed using NIH image 1.6 software.

Transmission electron microscopy

The diaphragms were fixed in 3% glutaraldehyde in 0.1 M cacodylate buffer (pH 7.4) for 1 h at 4 °C. The l diaphragms were then postfixed in 1% osmium tetroxide (pH 7.4), dehydrated in a graded series of ethanol, and embedded in EPON-812. Thin sections (70 nm) were cut, stained with uranyl acetate and lead citrate, and examined on a Hitachi H-7500 EM transmission electron microscope (Hitachi, Ltd., Tokyo, Japan).

Mitochondrial injury score

Mitochondrial injury was semi-quantitatively measured by using a scoring system that is based on the characteristic ultrastructural characteristics of mitochondria attendant to the progressive stages of cellular injury [2]. The severity of ultrastructural damage was quantified by determining a composite score (based on the scale of 0–5) that represented all the mitochondria visualized within the microscopy field. Score 0 = normal appearance. Score 1 = swelling of the endoplasmic reticulum, minimal mitochondrial swelling. Score 2 = mild mitochondrial swelling. Score 3 = moderate or focal high-amplitude swelling. Score 4 = diffuse high-amplitude swelling. Score 5 = high-amplitude swelling with mitochondrial flocculent densities or calcifications. An average number of 10 nonoverlapping fields in TEM of the diaphragm sections were analyzed for each section by a single investigator blinded to the mouse genotype.

Real-time PCR

For isolating total RNA, the lung tissues were homogenized in TRIzol reagents (Invitrogen Corporation, Carlsbad, CA, USA) according to the manufacturer's instructions. Total RNA (1 μg) was reverse transcribed by using a GeneAmp PCR system 9600 (PerkinElmer, Life Sciences, Inc., Boston, MA, USA), as previously described [35]. The following primers were used for real-time PCR: TRL4, forward primer 5′-CGCTTTCACCTCTGCCTTCACTACAG-3′ and reverse primer 5′-ACACTACCACAATAACCTTC CGGCTC-3′ and GAPDH as internal control, forward primer 5′-GGAGCGAGACCCCACTAACA-3′ and reverse primer 5′-ACATACTCAGCACCGGCCTC-3′ (Protech Technology Enterprise Co. Ltd., Taipei, Taiwan) [36, 37]. All quantitative PCR reactions using SYBR Master Mix were performed on a CFX96 Touch Real-Time PCR Detection system (Bio-Rad Laboratories, Inc., Hercules, CA, USA). All PCR reactions were performed in duplicate and heated to 95 °C for 5 min followed by 40 cycles of denaturation at 95 °C for 10 s, and annealing at 55 °C for 30 s. The relative gene expression was calculated using $2^{-\Delta\Delta CT}$ method and the standard curves (cycle threshold values versus template concentration) were prepared for each target gene and for the internal control (GAPDH) in each sample. The specific gene's cycle threshold (Ct) values were normalized to the GAPDH and compared with the nonventilated control group with LPS that was assigned a value of 1 to calculate the relative fold change in expression.

Statistical evaluation

The Western blots were quantitated using an NIH image analyzer Image J 1.27z (NIH, Bethesda, MD, USA) and presented as arbitrary units. Values were expressed as the mean ± SD from at least five separate experiments. The data of cross-sectional area, protein oxidation, MDA, total antioxidant capacity, superoxide dismutase, histopathologic assay, and oxygenation were analyzed using Statview 5.0 (Abascus Concepts, Cary, NC, USA; SAS Institute). All results of real-time PCR and Western blots were normalized to the nonventilated control wild-type mice with LPS. ANOVA was used to assess the statistical significance of the differences, followed by multiple comparisons with a Scheffe's test, and a P value <0.05 was considered statistically significant. We have performed the Shapiro-Wilk normality test and verify that all data are parametric (P >0.05).

Additional details, including TUNEL assay, were performed as described previously [2, 33].

Table 1 Physiologic conditions at the beginning and end of ventilation

	Nonventilated	Nonventilated + LPS	V_T 6 mL/kg + LPS	V_T 10 mL/kg + LPS	V_T 10 mL/kg + LPS + SN50	V_T 10 mL/kg + LPS + TLR4$^{-/-}$
PH	7.42 ± 0.05	7.39 ± 0.02	7.35 ± 0.07	7.39 ± 0.04	7.38 ± 0.05	7.36 ± 0.08
PaO2 (mmHg)	98.5 ± 0.2	96.2 ± 0.3	89.8 ± 0.4[a]	85.9 ± 3.1[a]	87.5 ± 2.4[a]	89.1 ± 2.1[a]
PaCO2 (mmHg)	39.2 ± 0.3	39.7 ± 0.2	38.9 ± 1.2	38.4 ± 1.5	37.5 ± 1.2	38.5 ± 1.4
MAP (mmHg)						
Start	85.4 ± 1.3	83.8 ± 0.6	85.0 ± 1.5	82.6 ± 2.8	84.8 ± 2.3	84.9 ± 1.7
End	85.0 ± 0.5	81.1 ± 0.3	79.0 ± 2.1[a]	75.5 ± 2.3[a]	78.2 ± 2.5[a]	79.1 ± 2.3[a]
PIP (mmHg)						
Start			15.9 ± 1.1	16.2 ± 1.4	15.8 ± 1.2	15.7 ± 1.3
End			16.9 ± 1.8	17.5 ± 1.9	17.1 ± 1.3	17.0 ± 1.4

At the end of the study period, we obtained the data of mean arterial pressure and arterial blood gases from the nonventilated control mice and mice ventilated at a tidal volume of 6 mL/kg or 10 mL/kg for 8 h ($n = 10$ per group). The normovolemic statuses of the mice were maintained by monitoring the mean artery pressure. Data are presented as means ± SDs

LPS lipopolysaccharide, *MAP* mean arterial pressure, *PIP* peak inspiratory pressure, *SN50* nuclear factor-κB inhibitor, *TLR4*$^{-/-}$ TLR4-deficient mice, V_T tidal volume

[a] Indicates that $P < 0.05$ when compared to the nonventilated control mice

Results

SN50 reduces the effects of MV on endotoxin-augmented VIDD, oxygen radicals, and inflammatory cytokines

We applied MV (6 mL/kg or 10 mL/kg) with room air for 8 h to induce VIDD in mice. The physiological conditions at the beginning and end of MV are listed in Table 1. The normovolemic status was maintained for the mice by monitoring their mean artery pressure. Because of rapid loss of diaphragm muscle strength and endurance, the washout of CO_2 by MV is balanced by impaired ventilation of the respiratory muscle. TEM was performed to examine MV- and LPS-induced alterations in the diaphragm ultrastructures. Compared with the mice subjected to V_T 6 mL/kg and the nonventilated control mice, those subjected to V_T 10 mL/kg demonstrated increased disruptions in diaphragmatic myofibrillar structures with tortured Z-bands and unclear A- and I-bands, mitochondrial swelling, and larger lipid droplets (Fig. 1a–d). Administration of SN50 substantially reduced damage to the diaphragmatic fibers (Figs. 1e). Recent studies have demonstrated the critical roles of MV-induced imbalances among inflammatory cytokines, oxidative loads, and antioxidant capacity in inducing VIDD [3, 12, 13, 18]. Increased levels of IL-6, MIP-2, protein carbonyl groups, and MDA, but reduced production of total antioxidant capacity and superoxide dismutase, were observed in mice subjected to MV with LPS when compared with those subjected to V_T 6 mL/kg and the nonventilated control mice (Fig. 2). However, a reversal of these characteristics was observed after the administration of SN50.

SN50 inhibits the effects of MV on endotoxin-enhanced atrogin-1, MuRF-1, and LC3-II expression

Western blot analyses were performed to identify the effects of MV on endotoxin-induced ubiquitin–proteosome and autophagy–lysosomal systems associated with VIDD. Total atrogin-1, MuRF-1, and LC3-II were upregulated in mice subjected to V_T 10 mL/kg compared with those subjected to V_T 6 mL/kg and the nonventilated control mice (Fig. 3). Administering SN50 substantially reduced the enhanced expression of atrogin-1, MuRF-1, and LC3-II by 10-mL/kg MV and endotoxin.

TLR4 homozygous knockout suppresses the effects of MV on endotoxin-augmented VIDD

TLR4-deficient mice were used to identify whether the beneficial effects provided by the administration of SN50 were mediated via the TLR4 pathway. The effects of MV (increase in oxidative stress; MIP-2 and IL-6 production; expression levels of atrogin-1, MuRF-1, caspase-3, and LC3-II; mitochondrial injury; and autophagosomes) in mice subjected to V_T 10 mL/kg with endotoxin were substantially attenuated in TLR4-deficient mice ($P < 0.05$; Figs. 4 and 5). However, the reduction of muscle fiber diameter and downregulation of P62, an indicator of autophagosome turnover, were highly restored in the TLR4-deficient mice ($P < 0.05$; Fig. 4). Furthermore, increases in diaphragmatic

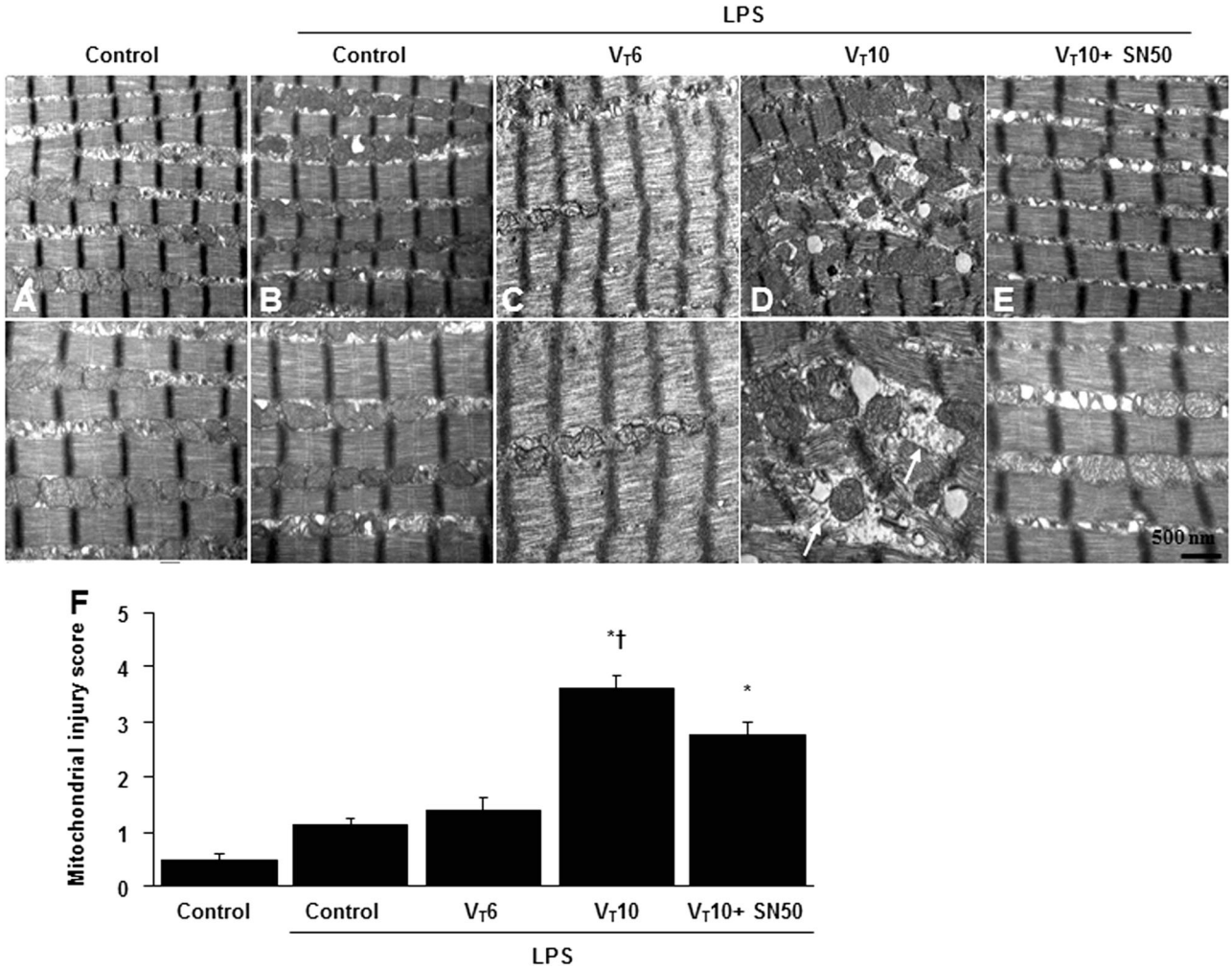

Fig. 1 Electron microscopy of the diaphragm. Representative micrographs of the longitudinal sections of diaphragm (×20,000: upper panel; ×40,000: lower panel) were from the same diaphragms of nonventilated control mice and mice ventilated at a tidal volume (V_T) of 6 mL/kg (V_T 6) or 10 mL/kg (V_T 10) for 8 h with or without LPS administration ($n = 3$ per group). **a**, **b** Nonventilated control wild-type mice with or without LPS treatment: normal sarcomeres with distinct A bands, I bands, and Z bands; **c** 6 mL/kg wild-type mice with LPS treatment: reduction of diaphragmatic disruption; **d** 10 mL/kg wild-type mice with LPS treatment: disruption of sarcomeric structure with loss of streaming of Z bands, mitochondrial swelling, and accumulation of lipid droplets; **e** 10 mL/kg wild-type mice pretreated with SN50: attenuation of diaphragmatic disruption. **f** Injury scores of lung mitochondria were from the diaphragms of nonventilated control mice and mice ventilated at a tidal volume of 6 mL/kg or 10 mL/kg for 8 h with or without LPS administration ($n = 3$ per group). Mitochondrial swelling with concomitant loss of cristae and autophagosomes containing heterogeneous cargo are identified by arrows. SN-50 2 mg/kg was given intraperitoneally 30 min before mechanical ventilation. $^*P < 0.05$ versus the nonventilated control mice with LPS treatment; $^\dagger P < 0.05$ versus all other groups. Scale bar represents 500 nm. LPS lipopolysaccharide

inflammation, oxidative stress, and mitochondrial damage were demonstrated in mice subjected to V_T 10 mL/kg with endotoxin compared with those subjected to V_T 10 mL/kg with normal saline and the nonventilated control mice (Figs. 4 and 5), suggesting the combinatorial effects of LPS treatment.

Because our study is a murine model of VIDD with mild endotoxemia, no statistically significant differences in these parameters were observed between the wild-type and TLR4-deficient nonventilated control mice with or without endotoxin (Figs. 4 and 5).

SN50 and TLR4 homozygous knockout suppress the effects of MV on endotoxin-exacerbated NF-κB activation and TLR4 expression

NF-κB has been demonstrated to play a crucial role in modulating the inflammatory responses of skeletal muscle fibers [3, 9, 19]. Western blot analyses were performed to identify the effects of MV on endotoxin-induced NF-κB activation in the diaphragm. We observed an upregulation of NF-κB phosphorylation in mice subjected to V_T 10 mL/kg compared with those subjected to V_T 6 mL/kg and the

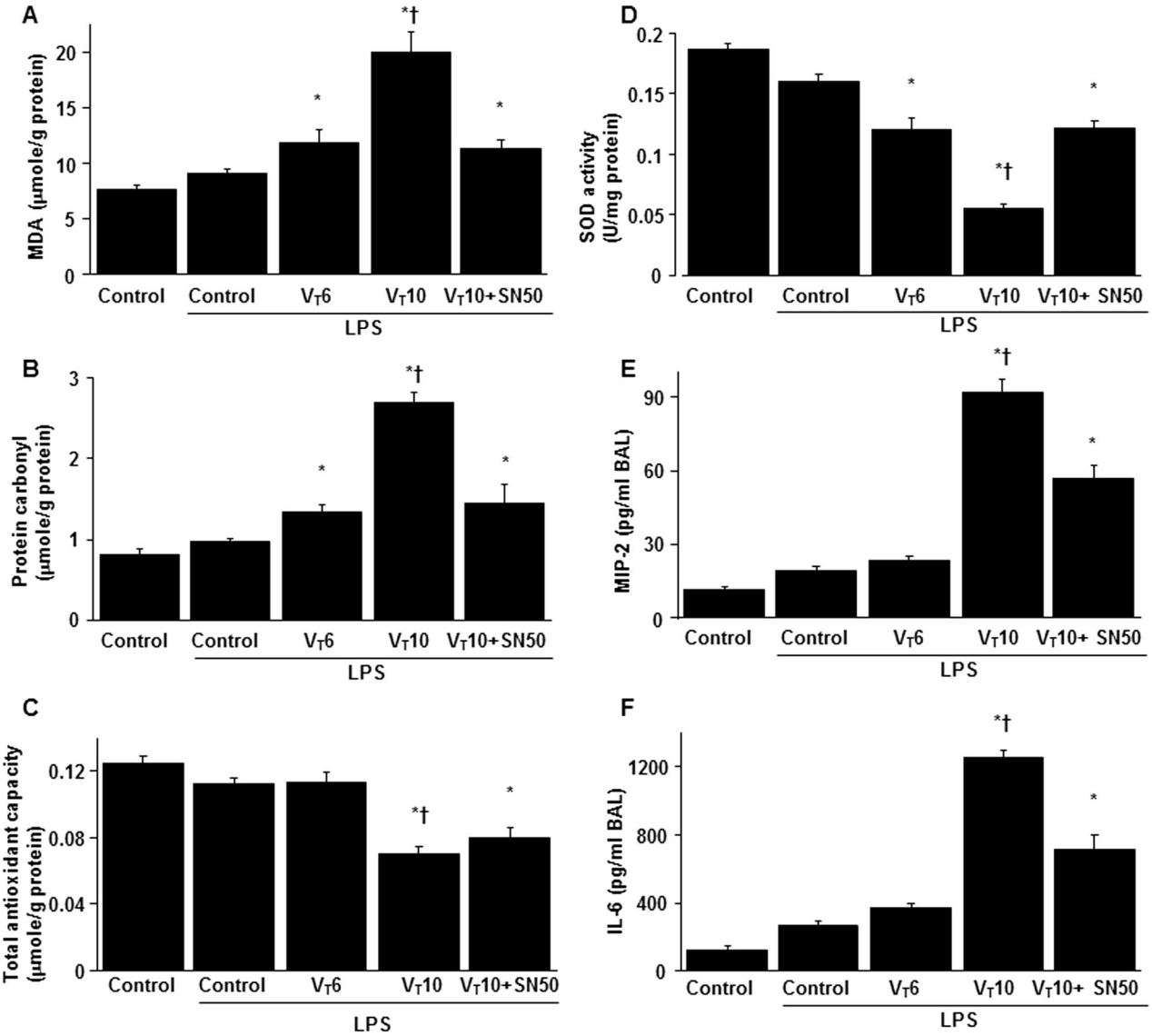

Fig. 2 SN50 suppressed endotoxin-augmented mechanical ventilation-mediated oxidative stress and inflammatory cytokines production. (**a**) MDA (diaphragm), (**b**) protein carbonyl groups (diaphragm), (**c**) total antioxidant capacity (diaphragm), (**d**) SOD (diaphragm), (**e**) BAL fluid MIP-2, and **f** BAL fluid IL-6 were from the nonventilated control mice and mice ventilated at a tidal volume of 6 mL/kg or 10 mL/kg for 8 h with or without LPS administration ($n = 5$ per group). SN-50 2 mg/kg was given intraperitoneally 30 min before ventilation. $^{*}P < 0.05$ versus the nonventilated control mice with LPS treatment; $^{\dagger}P < 0.05$ versus all other groups. BAL bronchoalveolar lavage, IL interleukin, MIP-2 macrophage inflammatory protein-2, MDA malondialdehyde, SOD sodium dismutase

nonventilated controls (Fig. 6a). Administration of SN50 substantially reduced the MV- and endotoxin-induced enhanced expression of NF-κB. Furthermore, the increased phosphorylation of IκBα was also reduced by SN-50 (Figs. 6b). TLR4 upregulation was reported to modulate VILI; therefore, we evaluated TLR4 expression to investigate the role of the TLR4 pathway in our VIDD model (Fig. 6c, d) [37]. Western blot analyses revealed increased TLR4 expression in mice subjected to V_T 10 mL/kg compared with those subjected to V_T 6 mL/kg and the nonventilated control mice. However, administration of SN50 did not reduce MV- and endotoxin-induced TLR4 expression, suggesting that TLR4 is an upstream regulator of NF-κB signaling involved in VIDD along with endotoxin (Fig. 6c). Immunohistochemistry was applied to further confirm the effects of TLR4 expression in endotoxin-induced VIDD (Fig. 4d). A substantial increase in the number of diaphragm muscle fibers positively stained for TLR4 was noted in mice subjected to V_T 10 mL/kg compared with those subjected to V_T 6 mL/kg and the nonventilated control mice. Consistent with the Western blot results, the increase in TLR4 activation after MV was substantially attenuated by TLR4 homozygous knockout.

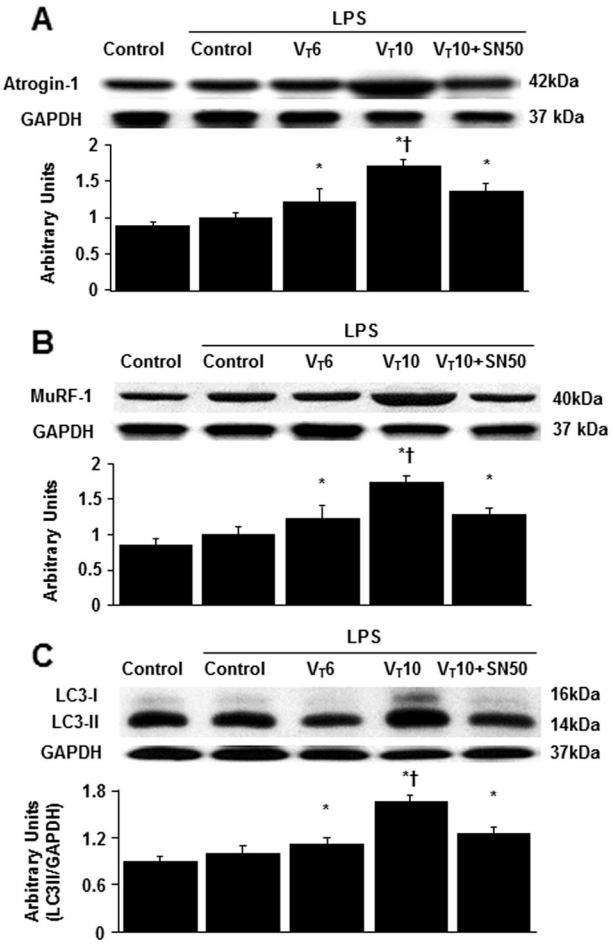

Fig. 3 SN50 abrogated endotoxin-augmented mechanical ventilation-induced atrogin-1, MuRF-1, and LC3-II expression in the diaphragm. Western blots were performed using antibodies that recognize atrogin-1 (**a**), MuRF-1 (**b**), LC3-II (**c**), and GAPDH expression from the diaphragms of nonventilated control mice and mice ventilated at a tidal volume of 6 mL/kg or 10 mL/kg for 8 h with or without LPS administration ($n = 5$ per group). Arbitrary units were expressed as relative atrogin-1, MuRF-1, and LC3-II activation ($n = 5$ per group). SN-50 2 mg/kg was given intraperitoneally 30 min before ventilation. $^{*}P < 0.05$ versus the nonventilated control mice with LPS treatment; $^{\dagger}P < 0.05$ versus all other groups. GAPDH glyceraldehydes-phosphate dehydrogenase, LC3-II light chain 3-II, MuRF-1 muscle ring finger-1

SN50 and TLR4 homozygous knockout reduce the effects of MV on endotoxin-enhanced expression of caspase-3 and diaphragm apoptosis

In addition to its role in VIDD, caspase-3 is vital for the intrinsic apoptotic pathway [6, 19]. Capase-3 expression was evaluated and TUNEL staining was performed to examine the roles of the caspase-3 pathway and apoptosis of diaphragm muscle fiber in endotoxin-related VIDD (Fig. 7). Caspase-3 activity was increased after 8 h of V_T 10 mL/kg MV compared with that in mice subjected to V_T 6 mL/kg and the nonventilated control mice. A significant increase in caspase-3 expression levels and the appearance of TUNEL-positive apoptotic nuclei in the murine diaphragm was observed in mice subjected to V_T 10 mL/kg with endotoxin compared with those subjected to V_T 10 mL/kg only (Figs. 7a, c). Notably, the increase in caspase-3 activity and MV- and endotoxin-exacerbated apoptosis in the murine diaphragm was ameliorated following the administration of SN50 as well as in the TLR4-deficient mice. Taken together, our results demonstrated that MV- and concurrent endotoxin-induced oxidative burst and the inflammatory responses in the diaphragm were prevented by the inhibition of the TLR4 and NF-κB pathways (Fig. 8).

Discussion

In clinical practice of critical care, patients with paradoxical respiration may need MV to let their respiratory muscles rest and make better control of sepsis. After well control of sepsis, they will be extubated as soon as possible. MV is a life-saving procedure for patients with ALI; however, controlled MV results in the rapid development of diaphragmatic weakness due to both muscle injury and atrophy. Animal studies have indicated that infection can induce significant diaphragm weakness in experimental models of sepsis [10–13, 18, 19]. A study of diaphragm strength in mechanically ventilated medical ICU patients demonstrated that the combination of ventilator-induced diaphragm inactivity and infection might produce sufficient diaphragm weakness to negatively influence patient outcomes and affect the duration of MV [7, 8]. Importantly, diaphragm weakness is a significant determinant for poor outcomes, including increased mortality and longer duration required for weaning in such populations of critically ill patients [7, 8, 38, 39]. Therefore, effective pharmacological treatments that improve diaphragm strength should be identified to reduce MV duration and ICU mortality. In the present study, we confirmed that pharmacologic inhibition of NF-κB can abrogate oxidative stress and enhance total antioxidant capacity; reduce inflammatory cytokine production and the activation of NF-κB signaling; attenuate muscle proteolysis, myonuclear apoptosis, mitochondrial dysfunction, and autophagy; and alleviate the atrophy of muscle fibers and mitochondrial dysfunction in a murine model of VIDD with endotoxemia. We further explored the role of TLR4 activation in regulating diaphragm injury through NF-κB signaling.

Diaphragm dysfunction during MV combined with sepsis can be exacerbated by mechanisms including increased ROS production, proinflammatory cytokine production, and increased proteolysis and autophagy [13]. The MV-induced release of proinflammatory mediators such as ROS and MIP-2 is involved in the pathogenesis of augmenting sepsis-induced systemic translocation and

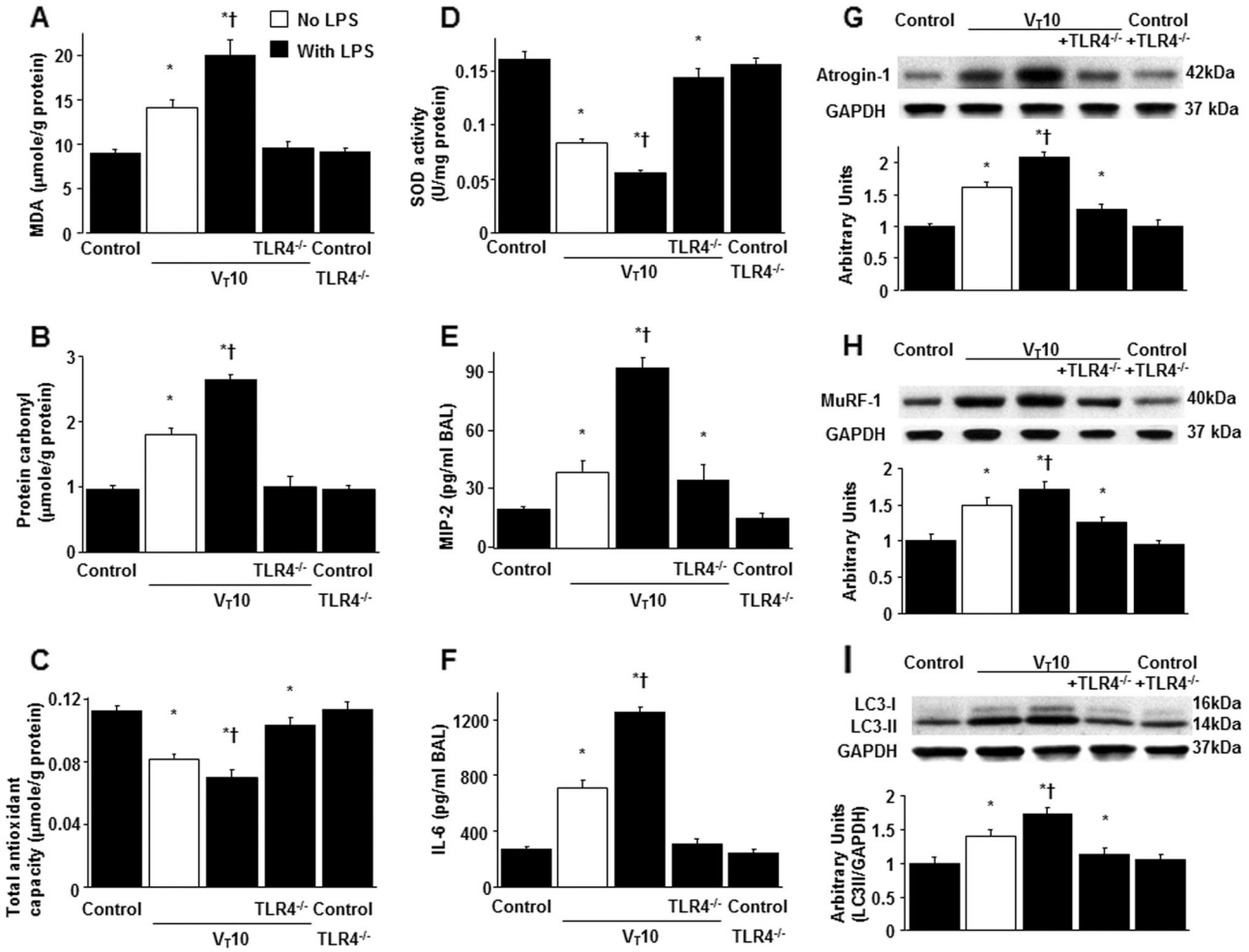

Fig. 4 Inhibition of endotoxin-augmented mechanical ventilation-mediated diaphragm dysfunction by TLR4 homozygous knockout. MDA (**a**), protein carbonyl groups (**b**), total antioxidant capacity (**c**), SOD (**d**), BAL fluid MIP-2 (**e**), BAL fluid IL-6 (**f**), and Western blots using antibodies that recognize atrogin-1 (**g**), MuRF-1 (**h**), LC3-II (**i**), and GAPDH expression were from the diaphragms of nonventilated control mice and mice ventilated at a tidal volume of 10 mL/kg for 8 h with or without LPS administration ($n = 5$ per group). Arbitrary units were expressed as relative atrogin-1, MuRF-1, and LC3-II expression ($n = 5$ per group). $^{*}P < 0.05$ versus the nonventilated control mice with LPS treatment; $^{\dagger}P < 0.05$ versus all other groups

diaphragm dysfunction [3]. Furthermore, IL-6 can exacerbate contractile dysfunctions of the diaphragm through mechanisms including decreased protein synthesis, induction of atrogin-1 and MuRF-1, and activation of the signal transducer and activator of transcription 3 (Stat3)-myostatin signaling pathway [13]. In the proteasome system of proteolysis, ubiquitin covalently binds to protein substrates and marks them for degradation. The binding of ubiquitin to the protein substrates requires specific ubiquitin protein ligase enzymes (E3). Crucially, the ubiquitin–proteasome system, consisting of a muscle-specific F-box protein atrogin-1 and a specific MuRF-1 class, degrades monomeric myofibrillar proteins that are released from sacromeric actomyosin complexes after digestion by calpain and caspase-3 [14, 17]. The results of the current study indicated that MV increased the production of IL-6, MIP-2, MDA, protein carbonyl groups, atrogin-1, and MuRF-1; furthermore, endotoxin aggravated the increase in lung inflammation and the associated skeletal muscle proteolysis.

NF-κB activation may play a specific role in triggering the inflammatory response of the skeletal myofibrils during endotoxemia and MV [3, 9, 19]. Previous animal studies employing transgenic mice have demonstrated that NF-κB signaling within the diaphragm muscle fibers is a key pathway leading to diaphragmatic weakness during acute endotoxemia, most likely through the effects on multiple proinflammatory mediators, oxidative stress, and proteolytic systems [9, 12]. MV-induced oxidative stress in the diaphragm is known to play a central role in the pathogenesis of VIDD, and occurs rapidly within the first 6 h of MV [10, 16, 22]. Oxidative stress is also pivotal in triggering several proteolytic pathways implicated in the initial disassembly of actomyosin complexes in the diaphragm and the activation of caspase-3 and NF-κB [19]. Caspase-3, a cysteine

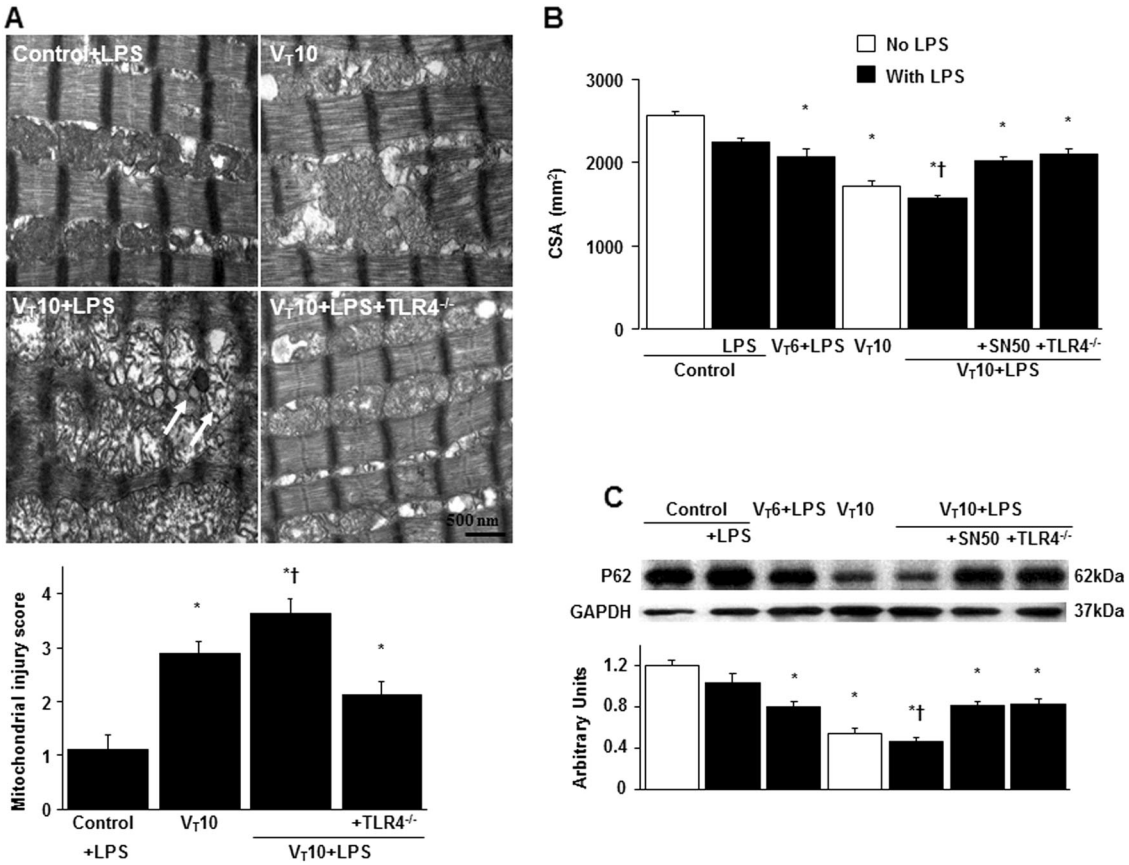

Fig. 5 Reduction of endotoxin-aggravated mechanical ventilation-induced diaphragm and mitochondrial injury by TLR4 homozygous knockout. **a** Representative micrographs of the longitudinal sections of diaphragm (×40,000) and quantification of mitochondrial injury were from the diaphragms of nonventilated control mice and mice ventilated at a tidal volume of 10 mL/kg for 8 h with or without LPS administration ($n = 3$ per group). Mitochondrial swelling with concomitant loss of cristae, vacuole formation, and autophagosomes containing heterogeneous cargo are identified by arrows. **b** Cross-sectional area of diaphragm muscle fiber was measured as described in Methods ($n = 5$ per group). **c** Western blots were conducted using an antibody that recognizes P62 expression and an antibody that recognizes GAPDH expression from the diaphragms of nonventilated control mice and mice ventilated at a tidal volume of 6 mL/kg or 10 mL/kg for 8 h with or without LPS administration ($n = 5$ per group). Arbitrary units were expressed as relative P62 and GAPDH expression ($n = 5$ per group).*$P < 0.05$ versus the nonventilated control mice with LPS treatment; $^{\dagger}P < 0.05$ versus all other groups

protease, can activate proapoptotic proteins to induce intrinsic apoptosis associated with mitochondria dysfunction [3, 9, 19, 29]. Moreover, NF-κB activation contributes to muscle atrophy because of its ability to transcribe specific atrophy-related genes and the muscle-specific ubiquitin E3 ligases, atrogin-1 and MuRF-1 [19]. Additionally, NF-κB activation enhanced LPS-induced autophagy in skeletal muscles. The influence of NF-κB on autophagy is highly dependent on cell type, cellular context, and the triggers for NF-κB activation [3]. Our data indicated that the combination of MV and endotoxemia upregulated the expression levels of NF-κB and caspase-3 and exacerbated myonuclear apoptosis. However, the upstream regulators of NF-κB in diaphragm damage remain to be elucidated.

The TLR family is composed of more than 10 pattern recognition receptors for the initiation of an inflammatory response. Different types of TLRs recognize different specific ligands, which include the microbial components and proteins released from the damaged tissue [4, 17, 18, 30–32]. Among them, TLR4 is probably the most thoroughly investigated, and it is crucial for the recognition of the lipid A moiety associated with microbial LPS [27, 30, 31]. Recent research demonstrated that the pulmonary inflammatory response to MV partly depends on TLR4 signaling [4, 18]. Activation of TLR4 is also expressed on muscle tissue, including the diaphragm in an animal model of sepsis [18]. Several studies have demonstrated that stimulation of TLR4 by LPS increases the expression of cytokines, such as IL-6, KC, and TNF-α, in the skeletal muscle [11–13, 20, 40]. Additionally, administration of the TLR4-specific ligand LPS to rodents elicits an upregulation of proinflammatory genes in the diaphragm and reduces the diaphragm strength. The activation of TLRs generally causes nuclear translocation of NF-κB and substantially elevates NF-κB luciferase reporter activity [6, 11, 30]. Moreover, interference with NF-κB activation during

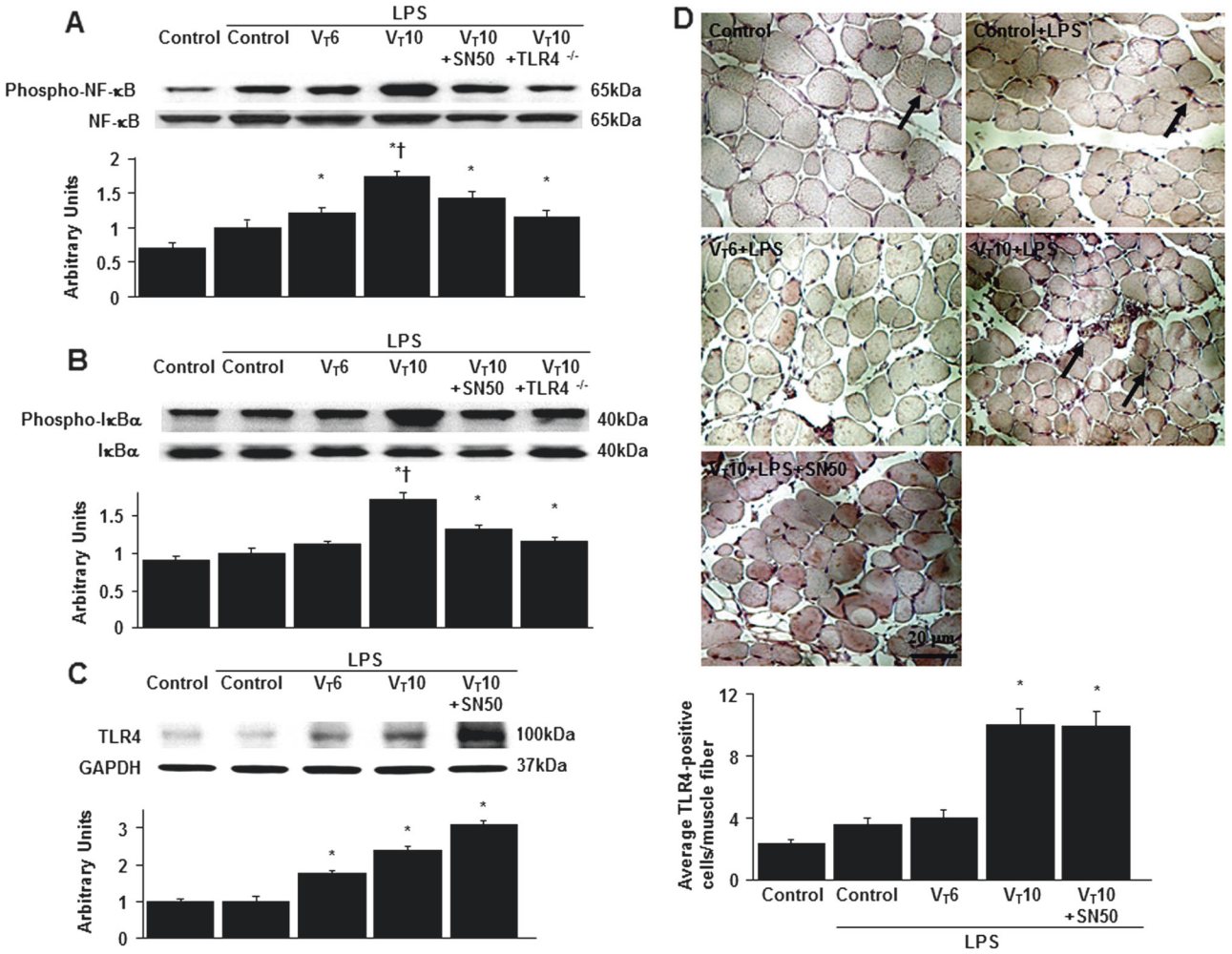

Fig. 6 SN50 and TLR4 homozygous knockout inhibited endotoxin-exacerbated mechanical ventilation-induced NF-κB activation and TLR4 expression. **a**, **b**, and **c** Western blots were conducted using antibodies that recognize the expression levels of phosphorylated NF-κB and IκBα and antibodies that recognize the expression levels of total NF-κB, IκBα, TRL4, and GAPDH from the diaphragms of nonventilated control mice and mice ventilated at a tidal volume of 6 mL/kg or 10 mL/kg for 8 h with or without LPS administration ($n = 5$ per group). Arbitrary units were expressed as relative NF-κB and TLR4 expression ($n = 5$ per group). **d** Representative micrographs (×400) with TRL4 staining of paraffin diaphragm sections and quantification were from the diaphragms of nonventilated control mice and mice ventilated at a tidal volume of 6 mL/kg or 10 mL/kg for 8 h with or without LPS administration ($n = 5$ per group). SN-50 2 mg/kg was given intraperitoneally 30 min before ventilation. A dark-brown diaminobenzidine signal identified by arrows indicates positive staining for TRL4 in the diaphragm, whereas shades of bluish tan signify nonreactive cells. $^{*}P < 0.05$ versus the nonventilated control mice with LPS treatment; $^{\dagger}P < 0.05$ versus all other groups. Scale bars represent 20 μm. Inhibitor-κBα IκBα, TLR4$^{-/-}$ TLR4-deficient mice

TLR4 stimulation is known to have greater inhibitory effects on chemokine gene expression [30].

Autophagy is a self-degradative process characterized by the removal of injured cellular components such as mitochondria in the skeletal muscles, and it is designed to maintain the growth, development, and quality of the mitochondrial networks [4, 6, 10, 11]. Mitochondria are a primary source of diaphragmatic ROS, a crucial upstream trigger that initiates the signaling events that lead to diaphragm myofibril atrophy after MV or during endotoxemia [6, 15, 28]. Although basal autophagy is important for maintaining cell survival, excessive autophagy induces pathological changes, such as muscle atrophy, intrinsic apoptosis, or cell death. Upregulation of LC3-II protein level has been described as a marker of increased autophagosome formation, whereas downregulation of p62 protein level is thought to be a marker of increased autophagic flux [6, 10]. By conjugating with phosphatidylethanolamin, LC3-I becomes a double-membraned autophagosome-bound LC3-II [11]. The accumulation of LC3-II in the diaphragm during MV could be primarily due to a pathological impairment of autophagosome degradation rather than upregulation of the autophagy pathway [10, 40]. In a recent study of sepsis, TLR4 activation increased autophagosome formation in a p38 MAPK-dependent manner [4]. In the current study, we observed that the combination of

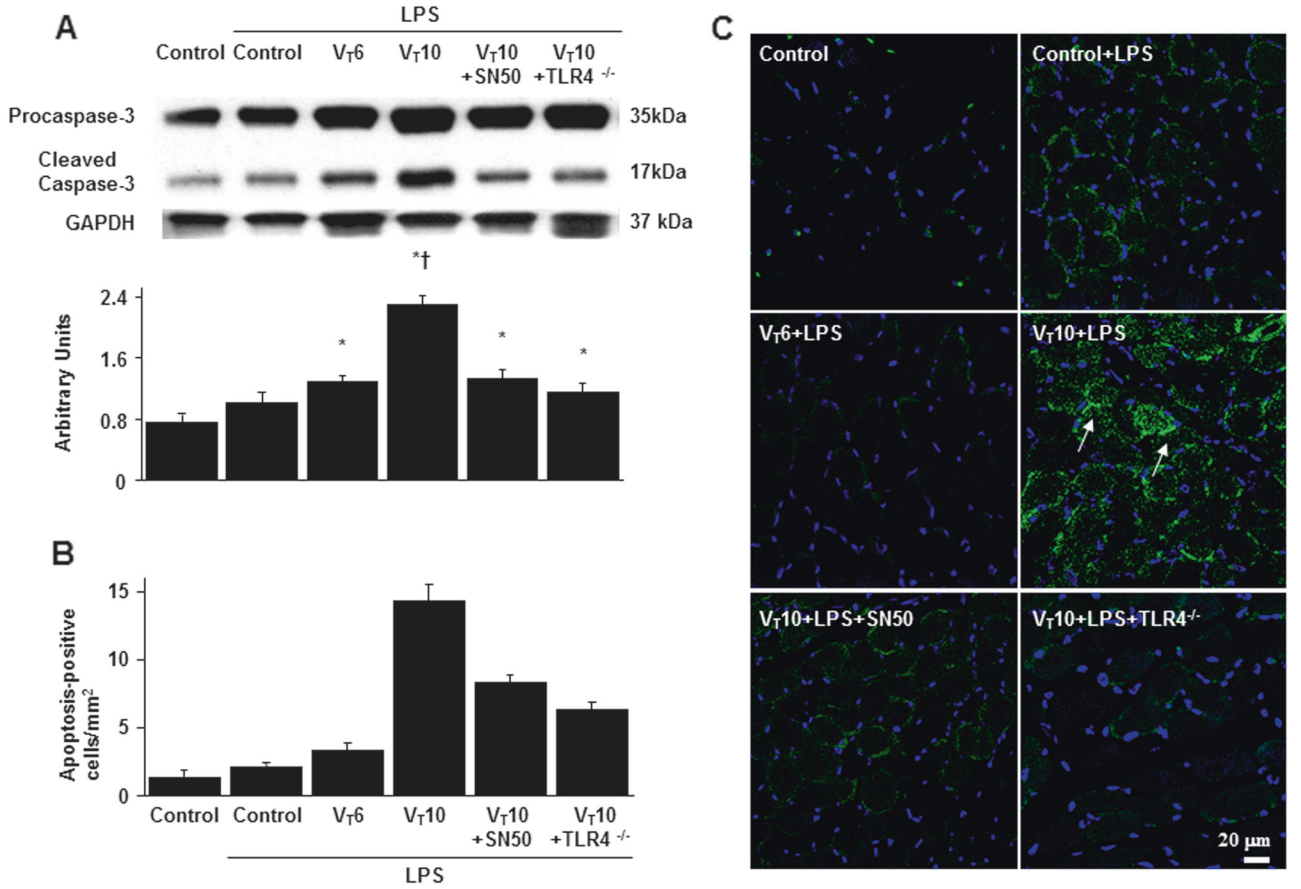

Fig. 7 SN50 and TLR4 homozygous knockout inhibited endotoxin-augmented mechanical ventilation-induced caspase-3 expression and apoptosis in the diaphragm. **a**, **b** Western blots were conducted using an antibody that recognizes caspase-3 expression and an antibody that recognizes the GAPDH expression from the diaphragms of nonventilated control mice and mice ventilated at a tidal volume of 6 mL/kg or 10 mL/kg for 8 h with or without LPS administration ($n = 5$ per group). Arbitrary units were expressed as the ratio of cleaved caspase-3 to GAPDH ($n = 5$ per group). **c** Representative micrographs (×400) with TUNEL staining of paraffin diaphragm sections and quantification were from the diaphragms of nonventilated control mice and mice ventilated at a tidal volume of 6 mL/kg or 10 mL/kg for 8 h with or without LPS administration ($n = 5$ per group). SN-50 2 mg/kg was given intraperitoneally 30 min before ventilation. Apoptotic cells are identified by arrows. A bright green signal indicates positive staining of apoptotic cells, and shades of dull green signify non-reactive cells. $^{*}P < 0.05$ versus the nonventilated control mice with room air; $^{\dagger}P < 0.05$ versus all other groups. Scale bars represent 20 μm. TUNEL terminal deoxynucleotidyl transferase-mediated dUTP-biotin nick end-labeling

MV and endotoxemia can induce autophagy, as confirmed by the presence of autophagosomes near the mitochondria through TEM analysis and the increased and decreased expression levels of LC3-II and P62, respectively. Mitochondrial dysfunction was also reflected by the high mitochondrial injury score, extensive swelling, deformed cristae, misfolding of the inner membrane, and the increase in lipid deposition indicating an increased influx of metabolic substrates into the muscle fibers in the diaphragm. TLR4 homozygous knockout can dampen the autophagy–lysosome pathway and alleviate mitochondrial ultrastructural changes by inhibiting TLR4/NF-κB signaling.

This study had a limitation. Tang et al. demonstrated that the Janus Kinase (JAK)-STAT pathway is involved in the pathogenesis of MV-induced oxidative stress and VIDD [41]. In our study, partial inhibition of diaphragm injury through TLR4 knockout or pharmacologic inhibition with SN50 suggested that TLR4/NF-κB signaling was only one of the many pathways contributing to VIDD. Additional experiments are necessary to investigate the other pathogenic signaling pathways.

In the present study, we determined that the administration of endotoxin enhanced MV-induced diaphragmatic oxidative stress, proteolysis, apoptosis, and autophagy, resulting in increased oxidative loads. In addition, atrogin-1, MuRF-1, caspase-3, and LC3-II expressions were increased, whereas P62 expression was reduced in a murine model of endotoxemia used to simulate an ICU clinical scenario. The negative effects of MV with endotoxemia on the diaphragm can be attenuated by pharmacologic inhibition with an NF-κB inhibitor or by TLR4 homozygous knockout, thus interrupting the TLR4/NF-κB pathway.

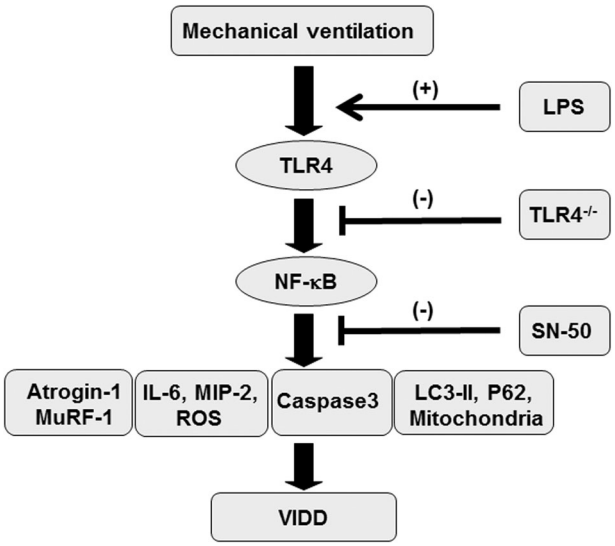

Fig. 8 Schematic figure illustrating the signaling pathway activation with mechanical ventilation and endotoxemia. Endotoxin-induced augmentation of mechanical stretch-mediated cytokine production and diaphragm damage were attenuated in TLR4-deficient mice. IL interleukin, LC3-II light chain 3-II, LPS lipopolysaccharide, MIP-2 macrophage inflammatory protein-2, MuRF-1 muscle ring finger-1, NF-κB nuclear factor-κB, ROS reactive oxygen species, TLR4 toll-like receptor 4, VIDD ventilator-induced diaphragm dysfunction

Knowledge of the combinatorial effects of mechanical forces and endotoxin on TLR4/NF-κB signaling might allow for the clarification of the pathophysiologic mechanisms that regulate VIDD in endotoxemia, which can necessitate long-term ventilator dependence and lead to poor outcomes. Furthermore, identification of the molecular mechanisms that regulate diaphragm injury is necessary for the advanced management of VIDD in patients with sepsis.

Acknowledgements The study was supported by the Ministry of Science and Technology (105-2314-B-182A-091-MY2). The funders had no role in study design, data collection and analysis, decision to publish, or preparation of the manuscript. The authors thank Chang-Hung Tien, Center for Big Data Analytics and Statistics, Laboratory Animal Center, and the Microscope Core Laboratory, Chang Gung Memorial Hospital, Linkou and Wallace Academic Editing, for their help with the experiment.

Compliance with ethical standards

Conflict of interest The authors declare that they have no conflict of interest.

References

1. Chacon-Cabrera A, Rojas Y, Martinez-Caro L, et al. Influence of mechanical ventilation and sepsis on redox balance in diaphragm, myocardium, limb muscles, and lungs. Transl Res. 2014;164:477–95.
2. Crouser ED, Julian MW, Blaho DV, et al. Endotoxin-induced mitochondrial damage correlates with impaired respiratory activity. Crit Care Med. 2002;30:276–84.
3. Demoule A, Divangahi M, Yahiaoui L, et al. Endotoxin triggers nuclear factor-kappaB-dependent up-regulation of multiple proinflammatory genes in the diaphragm. Am J Respir Crit Care Med. 2006;174:646–53.
4. Doyle A, Zhang G, Abdel Fattah EA, et al. Toll-like receptor 4 mediates lipopolysaccharide-induced muscle catabolism via coordinate activation of ubiquitin-proteasome and autophagy-lysosome pathways. FASEB J. 2011;25:99–110.
5. Jiang J, Yang B, Han G, et al. Early administration of cisatracurium attenuates sepsis-induced diaphragm dysfunction in rats. Inflammation. 2015;38:305–11.
6. Mofarrahi M, Sigala I, Guo Y, et al. Autophagy and skeletal muscles in sepsis. PLoS ONE. 2012;7:e47265.
7. Petrof BJ. Diaphragmatic dysfunction in the intensive care unit: caught in the cross-fire between sepsis and mechanical ventilation. Crit Care. 2013;17:R181.
8. Supinski GS, Callahan LA. Diaphragm weakness in mechanically ventilated critically ill patients. Crit Care. 2013;17:R120.
9. Okazaki T, Liang F, Li T, et al. Muscle-specific inhibition of the classical nuclear factor-kappaB pathway is protective against diaphragmatic weakness in murine endotoxemia. Crit Care Med. 2014;42:e501–9.
10. Azuelos I, Jung B, Picard M, et al. Relationship between autophagy and ventilator-induced diaphragmatic dysfunction. Anesthesiology. 2015;122:1349–61.
11. Hussain SN, Mofarrahi M, Sigala I, et al. Mechanical ventilation-induced diaphragm disuse in humans triggers autophagy. Am J Respir Crit Care Med. 2010;182:1377–86.
12. Jaber S, Petrof BJ, Jung B, et al. Rapidly progressive diaphragmatic weakness and injury during mechanical ventilation in humans. Am J Respir Crit Care Med. 2011;183:364–71.
13. Maes K, Stamiris A, Thomas D, et al. Effects of controlled mechanical ventilation on sepsis-induced diaphragm dysfunction in rats. Crit Care Med. 2014;42:e772–82.
14. Petrof BJ, Jaber S, Matecki S. Ventilator-induced diaphragmatic dysfunction. Curr Opin Crit Care. 2010;16:19–25.
15. Picard M, Azuelos I, Jung B, et al. Mechanical ventilation triggers abnormal mitochondrial dynamics and morphology in the diaphragm. J Appl Physiol. (1985).2015;118:1161–71.
16. Picard M, Jung B, Liang F, et al. Mitochondrial dysfunction and lipid accumulation in the human diaphragm during mechanical ventilation. Am J Respir Crit Care Med. 2012;186:1140–9.
17. Powers SK, Wiggs MP, Sollanek KJ, et al. Ventilator-induced diaphragm dysfunction: cause and effect. Am J Physiol Regul Integr Comp Physiol. 2013;305:R464–77.
18. Schellekens WJ, van Hees HW, Vaneker M, et al. Toll-like receptor 4 signaling in ventilator-induced diaphragm atrophy. Anesthesiology. 2012;117:329–38.
19. Smuder AJ, Hudson MB, Nelson WB, et al. Nuclear factor-kappaB signaling contributes to mechanical ventilation-induced diaphragm weakness. Crit Care Med. 2012;40:927–34.
20. Demoule A, Jung B, Prodanovic H, et al. Diaphragm dysfunction on admission to the intensive care unit. Prevalence, risk factors, and prognostic impact-a prospective study. Am J Respir Crit Care Med. 2013;188:213–9.
21. Powers SK, Smuder AJ, Fuller D, et al. CrossTalk proposal: mechanical ventilation-induced diaphragm atrophy is primarily due to inactivity. J Physiol. 2013;591:5255–7.
22. Zergeroglu MA,McKenzie MJ,Shanely RA, et al. Mechanical ventilation-induced oxidative stress in the diaphragm. J Appl Physiol (1985). 2003;95:1116–24.
23. McClung JM, Kavazis AN, Whidden MA, et al. Antioxidant administration attenuates mechanical ventilation-induced rat diaphragm muscle atrophy independent of protein kinase B (PKB Akt) signalling. J Physiol. 2007;585:203–15.

24. Jackman RW, Kandarian SC. The molecular basis of skeletal muscle atrophy. Am J Physiol Cell Physiol. 2004;287:C834–43.
25. McClung JM, Van Gammeren D, Whidden MA, et al. Apocynin attenuates diaphragm oxidative stress and protease activation during prolonged mechanical ventilation. Crit Care Med. 2009;37:1373–9.
26. Powers SK, Kavazis AN, DeRuisseau KC. Mechanisms of disuse muscle atrophy: role of oxidative stress. Am J Physiol Regul Integr Comp Physiol. 2005;288:R337–44.
27. Tadie JM, Bae HB, Jiang S, et al. HMGB1 promotes neutrophil extracellular trap formation through interactions with Toll-like receptor 4. Am J Physiol Lung Cell Mol Physiol. 2013;304: L342–9.
28. Powers SK, Hudson MB, Nelson WB, et al. Mitochondria-targeted antioxidants protect against mechanical ventilation-induced diaphragm weakness. Crit Care Med. 2011;39:1749–59.
29. Tang H, Lee M, Budak MT, et al. Intrinsic apoptosis in mechanically ventilated human diaphragm: linkage to a novel Fos/FoxO1/Stat3-Bim axis. FASEB J. 2011;25:2921–36.
30. Boyd JH, Divangahi M, Yahiaoui L, et al. Toll-like receptors differentially regulate CC and CXC chemokines in skeletal muscle via NF-kappaB and calcineurin. Infect Immun. 2006;74:6829–38.
31. Giordano C, Mojumdar K, Liang F, et al. Toll-like receptor 4 ablation in mdx mice reveals innate immunity as a therapeutic target in Duchenne muscular dystrophy. Hum Mol Genet. 2015;24:2147–62.
32. Zong M, Bruton JD, Grundtman C, et al. TLR4 as receptor for HMGB1 induced muscle dysfunction in myositis. Ann Rheum Dis. 2013;72:1390–9.
33. Li LF, Chang YL, Chen NH, et al. Inhibition of Src and forkhead box O1 signaling by induced pluripotent stem-cell therapy attenuates hyperoxia-augmented ventilator-induced diaphragm dysfunction. Transl Res. 2016;173:131–47 e131.
34. Li YY, Lee CH, Dedaj R, et al. High-molecular-weight hyaluronan- a possible new treatment for sepsis-induced lung injury: a preclinical study in mechanically ventilated rats. Crit Care. 2008;12:R102.
35. Li LF, Liu YY, Kao KC, et al. Mechanical ventilation augments bleomycin-induced epithelial-mesenchymal transition through the Src pathway. Lab Invest. 2014;94:1017–29.
36. Vitali R, Palone F, Cucchiara S, et al. Dipotassium glycyrrhizate inhibits HMGB1-dependent inflammation and ameliorates colitis in mice. PLoS ONE. 2013;8:e66527.
37. Gu Z, Chhabra AY, Alard P, et al. FcγRI is required for TGFβ2-treated macrophage-induced tolerance. Immunobiology. 2013; 218:1200–6.
38. Dres M, Goligher EC, Heunks LMA, et al. Critical illness-associated diaphragm weakness. Intensive Care Med. 2017;43: 1441–52.
39. Supinski GS, Morris PE, Dhar S, et al. Diaphragm Dysfunction in Critical Illness. Chest. 2018;153:1040–1051.
40. Tang H, Lee M, Khuong A, et al. Diaphragm muscle atrophy in the mouse after long-term mechanical ventilation. Muscle Nerve. 2013;48:272–8.
41. Tang H, Smith IJ, Hussain SN, et al. The JAK-STAT pathway is critical in ventilator-induced diaphragm dysfunction. Mol Med. 2014;20:579–89.